Novel mechanisms of type IV pilus regulation in *Acinetobacter baylyi*

Courtney K. Ellison[1,2*], Triana N. Dalia[3], Joshua W. Shaevitz[1*], Zemer Gitai[2*], and Ankur B. Dalia[3*]

1. Lewis-Sigler Institute for Integrative Genomics, Princeton University, Princeton, NJ
2. Department of Molecular Biology, Princeton University, Princeton, NJ
3. Department of Biology, Indiana University, Bloomington, IN

*Correspondence to: c.ellison@princeton.edu, shaevitz@princeton.edu, zgitai@princeton.edu, ankdalia@indiana.edu

Bacteria employ extracellular appendages called type IV pili (T4P) to interact with their environment. T4P are essential for diverse microbial behaviors including DNA uptake, surface sensing, virulence, protein secretion, and twitching motility[1]. While T4P have been studied extensively, our understanding of these nanomachines largely comes from work on a few model species. Here, we develop *Acinetobacter baylyi* as a new model organism to study T4P and uncover several unreported mechanisms of T4P regulation. First, using recently-developed T4P-labeling methods[2,3], we demonstrate that *A. baylyi* T4P are synthesized on one side of the cell body along the long axis of the cell, and we uncover that this pattern is dependent on components of a conserved chemosensory pathway. Second, we overturn the current dogma that T4P extension occurs through the action of a single, highly conserved ATP-hydrolyzing motor (ATPase) called PilB by showing that T4P synthesis in *A. baylyi* is dependent on two partially redundant and phylogenetically distinct motors, PilB and PilB2. Third, we uncover a small protein inhibitor of T4P synthesis that specifically inhibits PilB but not PilB2 activity. Together, these results demonstrate novel mechanisms of T4P regulation, which have broad implications for the unexplored diversity of T4P biology in microbial species.

T4P are thin, proteinaceous appendages that are broadly distributed throughout Bacteria and Archaea[4]. T4P are composed primarily of major pilin protein subunits that are polymerized or depolymerized through the activity of ATPases to mediate fiber extension and retraction, respectively[5]. T4P are subdivided into subcategories (generally T4aP, T4bP, and T4cP) based on protein homology and pilus function, with T4aP being the best-characterized. In the T4aP systems found in Gram-negative organisms, polymerization and depolymerization of pilins occurs through interactions of the extension ATPase PilB or retraction ATPase PilT with the

35 integral inner membrane platform protein PilC (Supplemental figure 1a). The growing fiber
36 spans an alignment complex from the inner membrane through the periplasm composed of
37 PilNOP to exit through the PilQ outer membrane secretin pore. Dynamic cycles of T4P
38 extension and retraction are critical for the diverse processes that these structures mediate
39 including twitching motility[6], surface sensing[2,7], virulence[8,9], and DNA uptake[10,11].
40 *Acinetobacter* species like *A. baumannii* and *A. nosocomialis* have recently become an
41 urgent medical threat due to their prevalence in hospital-acquired infections and their capacity to
42 acquire antibiotic resistance genes, a process that is achieved in part by T4aP-mediated DNA
43 uptake[12,13]. *Acinetobacter baylyi* is the most naturally transformable species reported to date[14],
44 with up to 50% of cells undergoing natural transformation in ideal settings. To study *A. baylyi*
45 T4P, we applied a recently-developed labeling method[2,3] by targeting the major pilin, ComP, for
46 cysteine substitution and subsequent labeling with thiol-reactive maleimide dyes. Maleimide-
47 labeling of the functional *comP*^{T129C} strain (Supplemental figure 1b) revealed an unusual pattern
48 of pilus synthesis, with T4P appearing only on one side of the cell body in a line along the long
49 axis of the cell (Figure 1a). Deletion of the retraction ATPase, PilT, resulted in hyperpiliated cells
50 exhibiting the same localization of T4P along the long axis of the cell. Cells with T4P facing the
51 microscope objective show T4P localize linearly along the side of the cell where they are
52 synthesized (Figure 1a). T4P localization has previously been shown to be polar or peritrichous
53 in other species, and to our knowledge, a long-axis localization pattern has not previously been
54 reported for any bacterial surface appendage or nanomachine.
55 Studies on the polarly localized T4P in *Pseudomonas aeruginosa*, a species closely
56 related to the *Acinetobacter* clade and one of the major model systems used to study T4P[1],
57 suggest that the chemosensory Pil-Chp system may play a role in controlling which pole of the
58 cell extends T4P[15]. The Pil-Chp system shares homology to flagellar chemotaxis systems, and
59 in *P. aeruginosa*, the methyl-accepting chemotaxis protein homologue, PilJ, is thought to signal
60 to the CheA homologue, ChpA. The CheW homologue, PilI is thought to act as a scaffold for Pil-
61 Chp signaling, leading to phosphoryl transfer from ChpA to the CheY homologues, PilG and
62 PilH to affect T4P synthesis. To determine whether the Pil-Chp system plays a role in controlling
63 where T4P are synthesized in *A. baylyi*, we made in-frame deletions of all Pil-Chp component
64 genes (Figure 1b). Deletion of *pilG*, *pilI*, and *chpA* all abrogated T4P localization and resulted in
65 the production of peritrichous T4P. However, deletions of *pilH* and, more surprisingly, *pilJ* did
66 not affect T4P patterning, suggesting that another inner membrane component may initiate
67 ChpA phosphoryl transfer in *A. baylyi* (Figure 1c, d). In *P. aeruginosa*, the scaffold protein FimV
68 interacts with the accessory protein FimL to recruit PilG to T4P machinery sites[16]. Although *A.*

69 *baylyi* lacks a FimV homologue, deletion of *fimL* also resulted in peritrichous pilus localization
70 (Figure 1c, d). In *P. aeruginosa*, T4P machinery is localized to both poles, but PilG is thought to
71 control which cell pole extends T4P[17,18]. However, an mCherry fusion to the outer membrane
72 secretin, PilQ, in *A. baylyi* demonstrated the same long-axis localization pattern as labeled T4P,
73 revealing a unique function for the Pil-Chp pathway in *A. baylyi* in regulating positioning of T4P
74 machinery and not simply regulating pilus dynamic activity (Supplemental figure 2).
75 Because PilG shares homology to two-component system response regulators, which
76 drive physiological changes downstream of an input signal, we hypothesized that PilG may
77 control the long-axis positioning of T4P machines. Consistent with this, we found that PilG-
78 mRuby3 localizes to the base of extended T4P (Supplemental figure 3a). Deletions of *pilI* and
79 *chpA* resulted in aberrant PilG-mRuby3 localization, mirroring T4P patterning in those mutants
80 (Figure 1e). The *fimL* mutant displayed cytoplasmic PilG signal, consistent with FimL playing a
81 role in PilG localization (Figure 1e). Notably, PilG-mRuby3 fluorescence intensity was
82 diminished in mutants with aberrant localization, suggesting a role for the Pil-Chp pathway in
83 controlling PilG levels (Supplemental figure 3b). The percent of cells making T4P in Pil-Chp
84 mutants was largely unchanged, suggesting an additional divergence from *P. aeruginosa* where
85 the Pil-Chp pathway also controls T4P production[19] (Supplemental figure 4a).
86 The Pil-Chp system is homologous to flagellar chemotaxis systems, so we suspected
87 that an external signal may feed into the Pil-Chp pathway to control T4P localization. Outer
88 membrane proteins in Gram-negative bacteria interface with the extracellular environment, and
89 we hypothesized that an outer membrane protein could influence the Pil-Chp system to regulate
90 T4P localization. To test this hypothesis, we deleted several outer membrane proteins
91 containing OmpA-like domains, and found that deletion of the major *ompA* gene, but not others,
92 resulted in peritrichous T4P localization (Figure 1c, d, Supplemental figure 5). Consistent with
93 an external signal feeding into the Pil-Chp pathway through OmpA, PilG-mRuby3 localization in
94 the *ompA* mutant displayed peritrichous localization similar to localization of labeled T4P (Figure
95 1d, e).
96 Because *A. baylyi* T4P participate in DNA uptake, we tested whether Pil-Chp mutants
97 with peritrichous localization were impacted for natural transformation. Surprisingly,
98 transformation was unaffected in mutants lacking Pil-Chp components (Supplemental figure 4b).
99 However, incubation of cells with fluorescently-labeled DNA resulted in co-localization of DNA
100 with T4P, which is consistent with the essential role of T4P-DNA binding during natural
101 transformation in *Vibrio cholerae*[11] (Figure 2a, Supplemental figure 4b). We reasoned that
102 natural transformation could be used to screen for other factors that regulate T4P in *A. baylyi*.

103 To that end, we performed a high throughput transposon-sequencing screen (Tn-seq) to identify
104 genes required for natural transformation. In this screen, loss of T4P-related genes resulted in
105 negative selection, indicating that they were critical for natural transformation as expected
106 (Figure 2b). To validate our Tn-seq results, we made in-frame deletions of representative genes
107 from each T4P-encoding operon, as well as genes known to be essential for natural
108 transformation that act downstream of T4P. Mutations in the T4P platform protein gene *pilC*, the
109 pilus regulatory gene *pilY1*, the outer membrane secretin gene *pilQ* and the retraction ATPase
110 gene *pilT* all showed a marked reduction in natural transformation, with most mutants exhibiting
111 transformation rates below our limit of detection (Figure 2c). T4P-labeling of *pilC*, *pilY1*, and *pilQ*
112 mutants revealed no visible T4P fibers (Figure 2d). Mutations in genes that act downstream of
113 T4P, including the periplasmic DNA-binding protein gene *comEA*, the inner membrane DNA-
114 transporter protein gene *comEC*, and the DNA-recombination helicase gene *comM* likewise
115 resulted in a reduction in transformation frequency, however, these strains still produced T4P
116 fibers as expected (Figure 2c, d).
117 We next sought to determine whether any of the previously uncharacterized genes from
118 our Tn-seq screen reduced natural transformation in *A. baylyi* by affecting T4P activity. Tn-seq
119 revealed that mutations in *pilB*, the canonical extension ATPase gene that is typically co-
120 transcribed with *pilC* and the pre-pilin peptidase, *pilD*, resulted in reduced natural transformation
121 (Figure 2b). However, we also found an additional *pilB* homologue, which we named *pilB2*, that
122 likewise exhibited lower rates of transformation (Figure 2b). Surprisingly, deletion of the
123 canonical *pilB* did not ablate transformation as would be expected based on homology to other
124 T4P[10] (Figure 3a). Mutation of *pilB2* only partially reduced transformation; however, natural
125 transformation was undetectable in the *pilB pilB2* double mutant (Figure 3a). T4P labeling in
126 *pilB*, *pilB2*, and *pilB pilB2* mutants revealed that all three mutants were defective in T4P
127 synthesis while *pilT* was intact. Strikingly, a *pilT* deletion, which prevents T4P retraction[20],
128 revealed that *pilB* mutant populations had similar numbers of cells producing T4P while *pilB2*
129 mutants were highly defective in T4P synthesis (Figure 3b, c). The *pilB pilB2 pilT* triple mutant
130 produced no detectable T4P fibers (Figure 3b, c). Together, these results indicate that both PilB
131 and PilB2 are essential for efficient T4P extension in *A. baylyi*, with PilB2 playing the dominant
132 role. Phylogenetic analysis of PilB2 homologues found among Gammaproteobacteria[4,21], which
133 include members of the PilT/VirB11 family of secretion ATPases, revealed that PilB2 clusters
134 with a group of proteins that are phylogenetically distinct from the canonical PilB ATPase
135 (Figure 3d, Supplemental figure 6). PilB and PilB2 proteins are as divergent from one another
136 as PilB and the type II secretion system proteins XcpR/GspE, or PilB and the MshE motors that

137 drive mannose-sensitive haemagglutinin (MSHA) pilus synthesis, suggesting that PilB2 evolved
138 as a functionally divergent class of proteins that is distinct from canonical PilB extension motors.
139 These results suggest that proteins that cluster with PilB2 may play similar functions in other
140 bacterial species and that multiple extension ATPases may be a common feature of diverse
141 T4P.

142 In addition to revealing the importance of PilB2 in T4P synthesis, our Tn-seq results also
143 uncovered an uncharacterized transcriptional regulator belonging to the XRE-family of
144 transcriptional repressors that is critical for natural transformation (Figure 2b, Figure 4a).
145 Deletion of this regulator, named *cpiR* for competence pilus inhibition repressor, resulted in a
146 100-fold reduction in transformation (Figure 4b). We hypothesized that CpiR repressed a factor
147 that inhibits natural transformation. Transcriptional repressors are often transcribed immediately
148 adjacent to the genes they repress. We thus deleted the upstream gene, named *cpiA* for
149 competence pilus inhibition actuator (Figure 4a), and found that transformation frequency was
150 restored in the *cpiR cpiA* double mutant background (Figure 4b). Expression of *cpiA* under the
151 control of an IPTG-inducible promoter (P_{tac}) was sufficient to reduce transformation frequency
152 even in the presence of *cpiR*, further suggesting that CpiR represses *cpiA* transcription.
153 Furthermore, we found that CpiR was sufficient to repress the *cpiA* promoter (using a P_{cpiA}-GFP
154 reporter) in the heterologous host *Vibrio cholerae*, which suggests that CpiR is a direct
155 repressor of P_{cpiA} (Figure 4c). Finally, we found that CpiA protein is only produced in a *cpiR*
156 mutant (Figure 4d). These results demonstrate that under lab conditions, CpiR represses *cpiA*
157 transcription to allow for high rates of natural transformation; however, in the absence of CpiR,
158 CpiA is produced and natural transformation is inhibited ~100-fold.

159 We next sought to determine the mechanism of transformation inhibition by CpiA.
160 Labeling of T4P in a *cpiR* mutant (when CpiA is expressed) revealed that cells were deficient in
161 T4P synthesis (Figure 4e). This defect was dependent on *cpiA* because piliation was restored in
162 the *cpiR cpiA* double mutant (Figure 4e). Deletion of *pilT* restored T4P synthesis in the *cpiR*
163 mutant (i.e. the *cpiR pilT* double mutant) (Figure 4e, f). This phenotype was reminiscent of the
164 restoration of piliation observed in the *pilB pilT* double mutant, and we hypothesized that CpiA
165 may regulate natural transformation by inhibiting PilB.

166 To test this hypothesis, we made *pilB cpiR* and *pilB2 cpiR* double mutants. T4P
167 synthesis was unaffected in *pilB cpiR pilT* (where PilB2 is the sole extension ATPase present),
168 while no T4P were detected in *pilB2 cpiR pilT* (where PilB is the sole extension ATPase
169 present) (Figure 4e, f). The defect in T4P synthesis in the *pilB2 cpiR pilT* strain was restored
170 when *cpiA* was deleted in this background, demonstrating that CpiA acts as a PilB inhibitor to

171 control natural transformation (Figure 4e, f). Transformation frequency assays corroborated
172 these results by demonstrating that deletion of *cpiR* only inhibited transformation in the *pilB2*
173 mutant background (where PilB is the sole extension ATPase) and not the *pilB* mutant
174 background (where PilB2 is the sole extension ATPase) (Figure 4g).
175 Environmental conditions play an integral role in regulating how bacteria respond to and
176 interact with their surroundings. The novel mechanisms of T4P regulation identified here are
177 likely a reflection of how environmental conditions influence bacterial physiology. Many bacteria
178 use chemotaxis systems to sense and respond to changes in environmental signals[22]. By
179 homology, an external cue likely controls T4P localization through the Pil-Chp pathway. Indeed,
180 the dependence of T4P localization on the outer membrane protein OmpA supports this idea, as
181 OmpA is a juncture for intracellular components and extracellular media. These data
182 demonstrate a novel role for OmpA in addition to its role in cell envelope integrity and virulence
183 as shown in other *Acinetobacter* species[23], highlighting its versatility in adapting to variable
184 environmental contexts. Future work will involve identifying the external signals that feed into
185 the Pil-Chp pathway through OmpA to control localization as well as the molecular mechanism
186 underlying T4P localization and the role it plays in the physiology of *Acinetobacter* species.
187 The acquisition of the additional extension motor PilB2 and the PilB-specific inhibitory
188 protein CpiA also likely resulted from a need to modulate T4P synthesis under different
189 environmental conditions. Bacteria generally limit T4P synthesis to environments where they
190 provide a selective advantage. For example, in *V. cholerae*, the production of T4a competence
191 pili requires chitin and quorum sensing[24], which are environmental conditions where cells are
192 likely to encounter other bacterial cells for horizontal gene transfer; while the T4b toxin-
193 coregulated (TCP) pili required for intestinal colonization are produced in response to host-
194 specific cues[25]. In *A. baylyi*, both PilB and PilB2 are required for T4P extension and,
195 consequently, efficient natural transformation. While CpiA is not expressed under laboratory
196 conditions (due to CpiR repression), it is possible that different environmental conditions
197 derepress *cpiA* to decrease pilus activity.
198 These results establish *A. baylyi* as a new model system to study T4P. By uncovering
199 several unknown mechanisms of T4P regulation, these studies underscore the unexplored
200 versatility and diversity of these ubiquitous systems and further highlight the need for new model
201 species to study T4P biology.
202
203 **Methods**
204 Bacterial strains and culture conditions

205 *Acinetobacter baylyi* strain ADP1 was used throughout this study. For a list of strains
206 used throughout, see Supplementary Table 1. *A. baylyi* cultures were grown at 30 °C in Miller
207 lysogeny broth (LB) medium and on agar supplemented with kanamycin (50 µg/mL),
208 spectinomycin (60 µg/mL), gentamycin (30 µg/mL), and/or chloramphenicol (30 µg/mL),
209 rifampicin (30 µg/mL), and/or streptomycin (10 µg/mL) as appropriate.
210
211 Construction of mutant strains
212 Mutants in *A. baylyi* were made using natural transformation as described previously.
213 Briefly, mutant constructs were made by splicing-by-overlap (SOE) PCR to stich 1) ~3 kb of the
214 homologous region upstream of the gene of interest, 2) the mutation where appropriate (for
215 deletion by allelic replacement with an antibiotic resistance cassette, or the fusion protein), and
216 3) the downstream region of homology. For a list of primers used to generate mutants in this
217 study, see Supplementary Table 2. The upstream region was amplified using F1 + R1 primers,
218 and the downstream region was amplified using F2 + R2 primers. All antibiotic resistance (AbR)
219 cassettes were amplified with ABD123 (ATTCCGGGGATCCGTCGAC) and ABD124
220 (TGTAGGCTGGAGCTGCTTC). Fusion proteins were amplified using the primers indicated in
221 Supplementary Table 2. In-frame deletions were constructed using F1 + R1 primer pairs to
222 amplify the upstream region and F2 + R2 primer pairs to amplify the downstream region with
223 ~20 bp homology to the remaining region of the downstream region built into the R1 primer and
224 ~20 bp homology to the upstream region built into the F2 primer. SOE PCR reactions were
225 performed using a mixture of the upstream and downstream regions, and middle region where
226 appropriate using F1 + R2 primers. SOE PCR products were added with 50 µl of overnight-
227 grown culture to 450 µl of LB in 2 ml round-bottom microcentrifuge tubes (USA Scientific) and
228 grown at 30 °C rotating on a roller drum for 1-3 hours. For AbR-constructs, transformants were
229 diluted out to 10^{-6} and dribble plated on LB and LB + AbR. For in-frame deletions and protein
230 fusion constructs, after the three-hour incubation, cells were incubated with 10 µl of DNaseI
231 (New England Biolabs) for 5 min at room temperature before 450 µl of LB was added.
232 Transformations were grown for an additional hour before cells were diluted and 100 µl of 10^{-6}
233 dilution was plated on LB plates. In-frame deletions were confirmed by PCR using primers ~150
234 bp up and downstream of the introduced mutation, and fusions were confirmed by sequencing.
235 Mutants in *V. cholerae* were made by chitin-induced natural transformation exactly as
236 previously described[26,27]. SOE products were generated exactly as described above. The
237 chromosomally integrated P_{BAD} ectopic expression construct is described in detail in ref [28].
238

239 Natural transformation assays

240 Assays were performed exactly as previously described[29]. Briefly, strains were grown
241 overnight in LB broth at 30°C rolling. Then, ~10^8 cells were subcultured into fresh LB medium
242 and 100 ng of tDNA was added. In this study, a ΔACIAD1551::$Spec^R$ PCR product (with 3kb
243 arms of homology) was used as the tDNA. Reactions were incubated with end-over-end rotation
244 at 30°C for 5 hours and then plated for quantitative culture on spectinomycin plates (to quantify
245 transformants) and on plain LB plates (to quantify total viable counts). Data are reported as the
246 transformation frequency, which is defined as the (CFU/mL of transformants) / (CFU/mL of total
247 viable counts).

248

249 Tn-seq Analysis

250 Transposon mutant libraries of *A. baylyi* were generated by electroporation of cells with
251 pDL1093, a vector that allows for Kan^R mini-Tn10 mutagenesis[30,31], and plating on kanamycin
252 plates. Approximately 100,000 Tn mutants were scraped off of plates and pooled to generate
253 the input transposon mutant library. This mutant library was then subjected to natural
254 transformation in three separate replicates exactly as described above using three different
255 sources of tDNA: a ΔACIAD1551::$Spec^R$ PCR product, an RpsL K43R (Sm^R) PCR product, or
256 an RpoB PCR product from a spontaneous rifampicin resistant mutant. Following incubation
257 with tDNA, reactions were split and outgrown in selective medium overnight (i.e. with the
258 appropriate antibiotic added to select for transformants = “transformant pool”) or grown
259 overnight in nonselective medium (i.e. in plain LB medium = “total pool”). Sequencing libraries of
260 the transposon-genomic junctions were generated for the Illumina platform using HTM-PCR
261 exactly as previously described[31,32]. Sequencing data were mapped to the *V. cholerae* N16961
262 genome[33] and the relative abundance of Tn insertions in all samples was determined on the
263 Galaxy platform[34]. Comparative analyses for Tn-seq were performed treating the "transformant
264 pool” as the output and the “total pool” as the input to determine genes that were over and
265 underrepresented following selection for transformants. Gene fitness was only assessed if a
266 gene contained at least 1 transposon insertion in at least two out of the three replicates of the
267 “total pool” samples. Also, the normalized abundance of insertions within a gene had to be
268 greater than 0.01 in the “total pool” when averaged across all three replicates (where 1 is the
269 expected normalized abundance for a “neutral” gene). These cutoffs allowed us to assess the
270 phenotype of ~83% of the genes (2747/3310) in the *A. baylyi* ADP1 genome. For visualization,
271 the relative abundance of Tn insertions within each gene is plotted from the “transformant pool”
272 relative to the “total pool”.

273

274 Pilin labeling, imaging, and quantification

275 Pilin labeling was performed as described previously with some changes[2,3]. Briefly, 100
276 µl of overnight-grown cultures was added to 900 µl of LB in 1.5 ml microcentrifuge tube, and
277 cells were grown at 30 °C rotating on a roller drum for 70 min. Cells were then centrifuged at
278 18,000 x *g* for 1 min and then resuspended in 50 µl of LB before labeling with 25 µg/ml of
279 AlexaFluor488 C_5-maleimide (AF488-mal) (ThermoFisher) for 15 min at room temperature.
280 Labeled cells were centrifuged, washed once with 100 µl of LB without disrupting the pellet, and
281 resuspended in 5-20 µl LB. Cell bodies were imaged using phase contrast microscopy while
282 labeled pili were imaged using fluorescence microscopy on a Nikon Ti-2 microscope using a
283 Plan Apo 100X objective, an FITC filter cube for pili, an mCherry filter cube for mRuby3 and
284 mCherry fusions, a Hamamatsu ORCAFlash4.0 camera, and Nikon NIS Elements Imaging
285 Software. Cell numbers and the percent of cells making pili were quantified manually using
286 ImageJ[35]. Cells were considered to have "mislocalized pili" if at least two pili were on opposing
287 sides of the cell. All imaging was performed under 1% UltraPure agarose (Invitrogen) pads
288 made with phosphate-buffered saline (PBS) solution.

289

290 Western blotting

291 Western blot analysis was performed exactly as previously described[36]. Briefly, cells
292 from overnight cultures were concentrated to an OD_{600} of 20. Then, cells were lysed on a
293 FastPrep-24 classic instrument at 4°C, and then clarified by centrifugation. Lysates were then
294 mixed with an equal volume of 2× SDS-PAGE sample buffer (220 mM Tris, pH 6.8, 25%
295 glycerol, 1.2% SDS, 0.02% bromophenol blue, and 5% β-mercaptoethanol) and boiled. Proteins
296 were separated on a 15% SDS polyacrylamide gel by SDS electrophoresis, electrophoretically
297 transferred to a polyvinylidene difluoride (PVDF) membrane, and probed with rabbit polyclonal
298 α-FLAG antibodies (Sigma Aldrich) or mouse monoclonal α-RpoA (BioLegend) primary
299 antibodies. Blots were then incubated with α-rabbit or α-mouse horseradish peroxidase (HRP)-
300 conjugated secondary antibodies, developed using Pierce ECL Western blotting substrate
301 (Thermo Fisher), and imaged on a Protein Simple FluorChem E instrument.

302

303 Measuring GFP fluorescence in reporter strains

304 *V. cholerae* reporter strains harboring P_{cpiA}-GFP were grown to late log in LB medium
305 with or without 0.2% arabinose as indicated. Cells were then washed once in instant ocean
306 medium (7g/L; Aquarium Systems) and transferred to a 96-well plate. Fluorescence was then

307 determined on a Biotek H1M plate reader with monochromater set to 500 nm for excitation and
308 540 nm for emission.
309
310 Fluorescent DNA binding/uptake
311 A ~7 kb PCR product was fluorescently labeled as described previously[11] using the Cy3
312 LabelIT kit (Mirus Biosciences) as per manufacturer recommendations. For the parent strain, 1
313 µl (100 ng) of Cy3-DNA was added to 900 µl of LB in a 1.5 ml microcentrifuge tube along with
314 100 µl of overnight-grown cultures, and cells were grown at 30°C rotating on a roller drum for 70
315 min. Pili were then labeled as described above.
316 To visualize DNA-binding in the *pilT* mutant, cells were grown as described above, but 1
317 µl (100 ng) of Cy3-DNA was added to cells along with AF488-mal and incubated for 25 min
318 before washing. Cells were imaged using the same microscopy setup described above, using a
319 dsRed filter cube to image Cy3-DNA.
320
321 Phylogenetic analysis
322 PilB2 homologues were identified by BLAST using 43 manually selected
323 Gammaproteobacteria genomes[37] through Integrated Microbial Genomes and Microbiomes
324 online resources (IMG)[38] resulting in 209 protein sequences. The FtsK protein from *A. baylyi*
325 ADP1 was added and used as an outgroup. Through the NGPhylogeny.fr server[39], sequences
326 were aligned using the default parameters of MAFFT[40], and phylogenetic tree construction was
327 performed on the aligned sequences using the default parameters of FastTree software[41,42] set
328 to perform 100 bootstraps[43]. The resulting tree was visualized using the Interactive Tree of Life
329 (iTOL) visualization software[44], from which trees were exported for publication.
330
331 **Acknowledgements**: We would like to thank E. Geisinger for *A. baylyi* ADP1 ATCC33305
332 wildtype strain, and we would like to thank K. Hummels and B. Bratton for helpful suggestions
333 on phylogenetic analysis. CKE is a Damon Runyon Fellow supported by the Damon Runyon
334 Cancer Research Foundation (DRG-2385-20). This work was supported in part by the National
335 Science Foundation, through the Center for the Physics of Biological Function (PHY-1734030).
336 This work was supported by grant R35GM128674 from the National Institutes of Health
337 awarded to ABD and the National Institutes of Health Pioneer Award 1DP1AI124669-01
338 awarded to ZG.
339

Author contributions: CKE and ABD designed and coordinated the overall study. CKE, TND, and ABD performed the experiments. All authors analyzed and interpreted data. CKE and ABD wrote the manuscript with help from ZG and JWS.

Competing interests: The authors declare no competing interests.

Data availability statement: The data that support the findings of this study are available from the corresponding authors upon request.

References

1. Burrows, L. L. Pseudomonas aeruginosa twitching motility: type IV pili in action. *Annu Rev Microbiol* **66**, 493–520 (2012).
2. Ellison, C. K. C. K. *et al.* Obstruction of pilus retraction stimulates bacterial surface sensing. *Science.* **358**, 535–538 (2017).
3. Ellison, C. K., Dalia, T. N., Dalia, A. B. & Brun, Y. V. Real-time microscopy and physical perturbation of bacterial pili using maleimide-conjugated molecules. *Nat. Protoc.* **14**, (2019).
4. Denise, R., Abby, S. S. & Rocha, E. P. C. Diversification of the type IV filament superfamily into machines for adhesion, protein secretion, DNA uptake, and motility. *PLOS Biol.* **17**, e3000390 (2019).
5. Craig, L., Forest, K. T. & Maier, B. Type IV pili: dynamics, biophysics and functional consequences. *Nat. Rev. Microbiol.* 1 (2019). doi:10.1038/s41579-019-0195-4
6. Merz, A. J., So, M. & Sheetz, M. P. Pilus retraction powers bacterial twitching motility. *Nature* **407**, 98–102 (2000).
7. Snyder, R. A. *et al.* Surface sensing stimulates cellular differentiation in Caulobacter crescentus. *Proc. Natl. Acad. Sci.* (2020). doi:10.1073/PNAS.1920291117
8. Siryaporn, A. *et al.* Surface attachment induces Pseudomonas aeruginosa virulence. *Proc. Natl. Acad. Sci.* **111**, 16860–16865 (2014).
9. Persat, A., Inclan, Y. F., Engel, J. N., Stone, H. A. & Gitai, Z. Type IV pili mechanochemically regulate virulence factors in *Pseudomonas aeruginosa*. *Proc. Natl. Acad. Sci.* **112**, 7563–7568 (2015).
10. Seitz, P. & Blokesch, M. DNA-uptake machinery of naturally competent Vibrio cholerae. *Proc. Natl. Acad. Sci. U. S. A.* **110**, 17987–92 (2013).
11. Ellison, C. K. *et al.* Retraction of DNA-bound type IV competence pili initiates DNA uptake during natural transformation in Vibrio cholerae. *Nat. Microbiol.* **3**, 773–780 (2018).
12. Harding, C. M. *et al.* Acinetobacter baumannii strain M2 produces type IV Pili which play a role in natural transformation and twitching motility but not surface-associated motility. *MBio* **4**, (2013).
13. Godeux, A. S. *et al.* Fluorescence-based detection of natural transformation in drug-resistant acinetobacter baumannii. *J. Bacteriol.* **200**, (2018).
14. Metzgar, D. *et al.* Acinetobacter sp. ADP1: An ideal model organism for genetic analysis and genome engineering. *Nucleic Acids Res.* **32**, 5780–5790 (2004).
15. Jain, R., Sliusarenko, O. & Kazmierczak, B. I. Interaction of the cyclic-di-GMP binding protein FimX and the Type 4 pilus assembly ATPase promotes pilus assembly. *PLOS Pathog.* **13**, e1006594 (2017).
16. Inclan, Y. F. *et al.* A scaffold protein connects type IV pili with the Chp chemosensory system to mediate activation of virulence signaling in Pseudomonas aeruginosa. *Mol. Microbiol.* **101**, 590–605 (2016).
17. Bertrand, J. J., West, J. T. & Engel, J. N. Genetic analysis of the regulation of type IV pilus function by the Chp chemosensory system of Pseudomonas aeruginosa. *J. Bacteriol.* **192**, 994–1010 (2010).
18. Carter, T. *et al.* The type IVa pilus machinery is recruited to sites of future cell division. *MBio* **8**, (2017).
19. Buensuceso, R. N. C. *et al.* Cyclic AMP-independent control of twitching motility in Pseudomonas aeruginosa. *J. Bacteriol.* **199**, (2017).
20. Chlebek, J. L. *et al.* PilT and PilU are homohexameric ATPases that coordinate to retract type IVa pili. *PLOS Genet.* **15**, e1008448 (2019).
21. McCallum, M., Tammam, S., Khan, A., Burrows, L. L. & Howell, P. L. The molecular mechanism of the type IVa pilus motors. *Nat. Commun.* **8**, 15091 (2017).

401 22. Wadhams, G. H. & Armitage, J. P. Making sense of it all: Bacterial chemotaxis. *Nature*
402 *Reviews Molecular Cell Biology* **5**, 1024–1037 (2004).
403 23. Gaddy, J. A., Tomaras, A. P. & Actis, L. A. The Acinetobacter baumannii 19606 OmpA
404 protein plays a role in biofilm formation on abiotic surfaces and in the interaction of this
405 pathogen with eukaryotic cells. *Infect. Immun.* **77**, 3150–3160 (2009).
406 24. Meibom, K. L., Blokesch, M., Dolganov, N. A., Wu, C.-Y. & Schoolnik, G. K. Chitin
407 Induces Natural Competence in Vibrio cholerae. *Science (80-.).* **310**, 1824–1827 (2005).
408 25. Schuhmacher, D. A. & Klose, K. E. Environmental signals modulate ToxT-dependent
409 virulence factor expression in Vibrio cholerae. *J. Bacteriol.* **181**, 1508–1514 (1999).
410 26. Dalia, A. B., McDonough, E. & Camilli, A. Multiplex genome editing by natural
411 transformation. *Proc. Natl. Acad. Sci. U. S. A.* **111**, 8937–42 (2014).
412 27. Dalia, A. B. Natural Cotransformation and Multiplex Genome Editing by Natural
413 Transformation (MuGENT) of Vibrio cholerae. in *Methods in molecular biology (Clifton,*
414 *N.J.)* **1839**, 53–64 (2018).
415 28. Dalia, T. N., Chlebek, J. L. & Dalia, A. B. A modular chromosomally integrated toolkit for
416 ectopic gene expression in Vibrio cholerae. *bioRxiv* 2020.03.02.973776 (2020).
417 doi:10.1101/2020.03.02.973776
418 29. Nero, T. M. *et al.* ComM is a hexameric helicase that promotes branch migration during
419 natural transformation in diverse Gram-negative species. *Nucleic Acids Res.* **46**, 6099–
420 6111 (2018).
421 30. Shull, L. M. & Camilli, A. Transposon sequencing of vibrio cholerae in the infant rabbit
422 model of cholera. in *Methods in Molecular Biology* **1839**, 103–116 (Humana Press Inc.,
423 2018).
424 31. Mcdonough, E., Lazinski, D. W. & Camilli, A. Identification of in vivo regulators of the
425 Vibrio choleraexds gene using a high-throughput genetic selection. *Mol. Microbiol.* **92**,
426 302–315 (2014).
427 32. Lazinski, D. W. & Camilli, A. Homopolymer tail-mediated ligation PCR: A streamlined and
428 highly efficient method for DNA cloning and library construction. *Biotechniques* **54**, 25–34
429 (2013).
430 33. Heidelberg, J. F. *et al.* DNA sequence of both chromosomes of the cholera pathogen
431 Vibrio cholerae. *Nature* **406**, 477–483 (2000).
432 34. Afgan, E. *et al.* The Galaxy platform for accessible, reproducible and collaborative
433 biomedical analyses: 2016 update. *Nucleic Acids Res.* **44**, W3–W10 (2016).
434 35. Schneider, C. A., Rasband, W. S. & Eliceiri, K. W. NIH Image to ImageJ: 25 years of
435 image analysis. *Nat. Methods* **9**, 671–675 (2012).
436 36. Klancher, C., Newman, J., Ball, A., van Kessel, J. & Dalia, A. Species-specific quorum
437 sensing represses the chitobiose utilization locus in Vibrio cholerae. *Appl. Environ.*
438 *Microbiol.* **86**, (2020).
439 37. Mukherjee, S. *et al.* Genomes OnLine database (GOLD) v.7: Updates and new features.
440 *Nucleic Acids Res.* **47**, D649–D659 (2019).
441 38. Chen, I. M. A. *et al.* IMG/M v.5.0: An integrated data management and comparative
442 analysis system for microbial genomes and microbiomes. *Nucleic Acids Res.* **47**, D666–
443 D677 (2019).
444 39. Lemoine, F. *et al.* NGPhylogeny.fr: New generation phylogenetic services for non-
445 specialists. *Nucleic Acids Res.* **47**, W260–W265 (2019).
446 40. Katoh, K. & Standley, D. M. MAFFT multiple sequence alignment software version 7:
447 Improvements in performance and usability. *Mol. Biol. Evol.* **30**, 772–780 (2013).
448 41. Price, M. N., Dehal, P. S. & Arkin, A. P. Fasttree: Computing large minimum evolution
449 trees with profiles instead of a distance matrix. *Mol. Biol. Evol.* **26**, 1641–1650 (2009).
450 42. Price, M. N., Dehal, P. S. & Arkin, A. P. FastTree 2 - Approximately maximum-likelihood
451 trees for large alignments. *PLoS One* **5**, e9490 (2010).

452 43. Lemoine, F. *et al.* Renewing Felsenstein's phylogenetic bootstrap in the era of big data.
453 *Nature* **556**, 452–456 (2018).
454 44. Letunic, I. & Bork, P. Interactive Tree of Life (iTOL) v4: Recent updates and new
455 developments. *Nucleic Acids Res.* **47**, W256–W259 (2019).
456

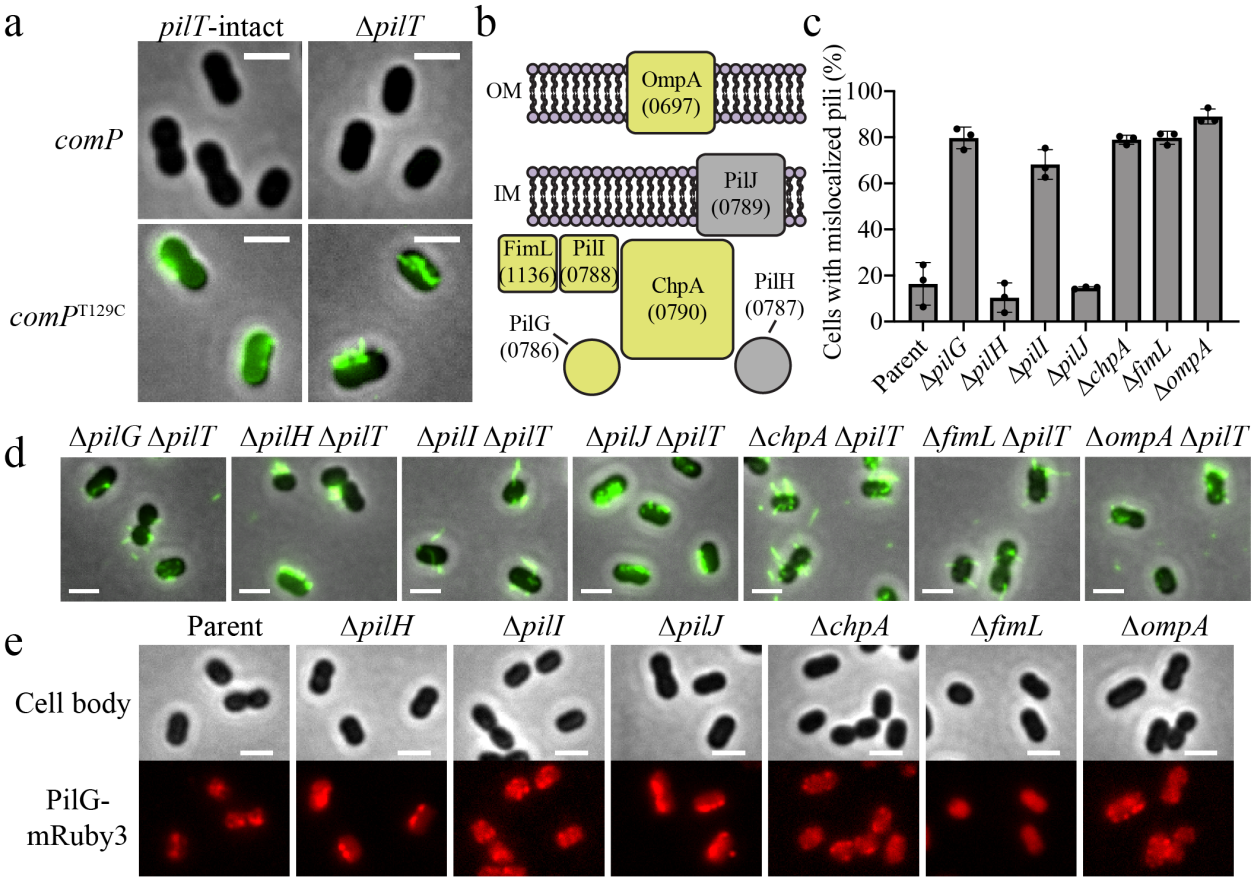

Figure 1. *A. baylyi* T4aP are produced in a line along the long axis of the cell body in a Pil-Chp dependent manner. (**a**) Representative images of indicated strains labeled with AF488-mal. (**b**) Schematic of the *A. baylyi* components of the Pil-Chp system. Deletion of tan proteins alters T4P localization, while deletion of the gray proteins does not. Numbers in parentheses are the ACIAD gene designations for each component. OM, outer membrane; IM, inner membrane. (**c**) Percent of piliated cells in *pilT* mutants with mislocalized T4P in indicated strains. Cells were determined to have "mislocalized pili" if they had at least two pili on opposing sides of the long axis of the cell body. Cells that only made one pilus were counted in the total number of piliated cells but were not counted as "mislocalized." Each data point represents an independent, biological replicate and bar graphs indicate the mean ± SD. For each biological replicate, a minimum of 70 total cells were assessed. (**d**) Representative images of indicated strains labeled with AF488-mal with background fluorescence subtracted. (**e**) Representative images of indicated PilG-mRuby3 strains with background fluorescence subtracted and fluorescence channel lookup tables adjusted to show PilG-mRuby3 localization. Scale bars, 2 μm.

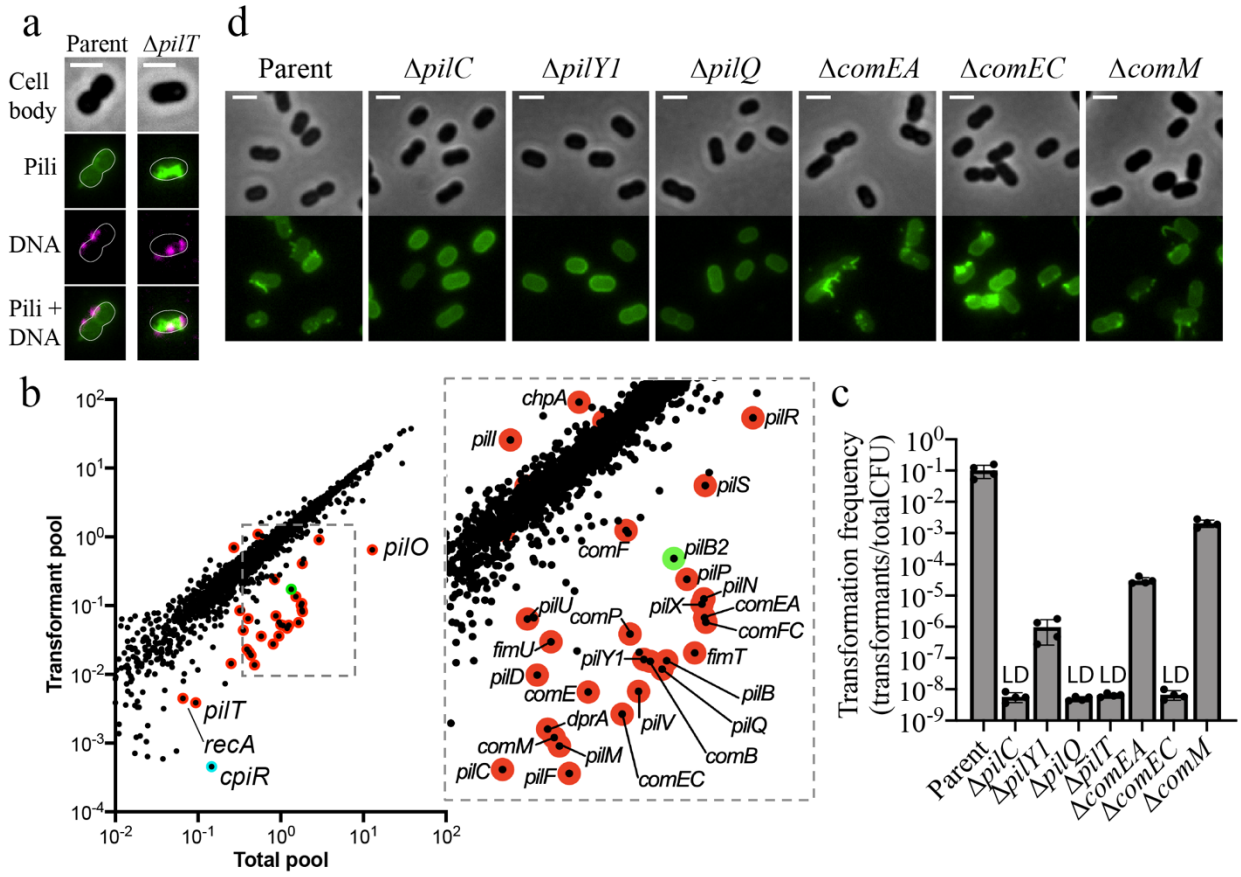

Figure 2. Tn-seq reveals factors important for natural transformation and T4P synthesis. (**a**) Representative images of cells with AF488-mal labeled pili incubated with fluorescently-labeled DNA. (**b**) Visual representation of Tn-seq screen showing the relative abundance of each gene in the "total pool" of transposon mutants compared to the "transformant pool" recovered after natural transformation. Known T4P regulatory genes are outlined in red. *pilB2* is outlined in green, and *cpiR* is outlined in cyan. (**c**) Natural transformation assays of indicated strains. Each data point represents a biological replicate and bar graphs indicate the mean ± SD. LD, limit of detection. (**d**) Representative images of strains from natural transformation assays shown in **c** labeled with AF488-mal. Scale bars, 2 μm.

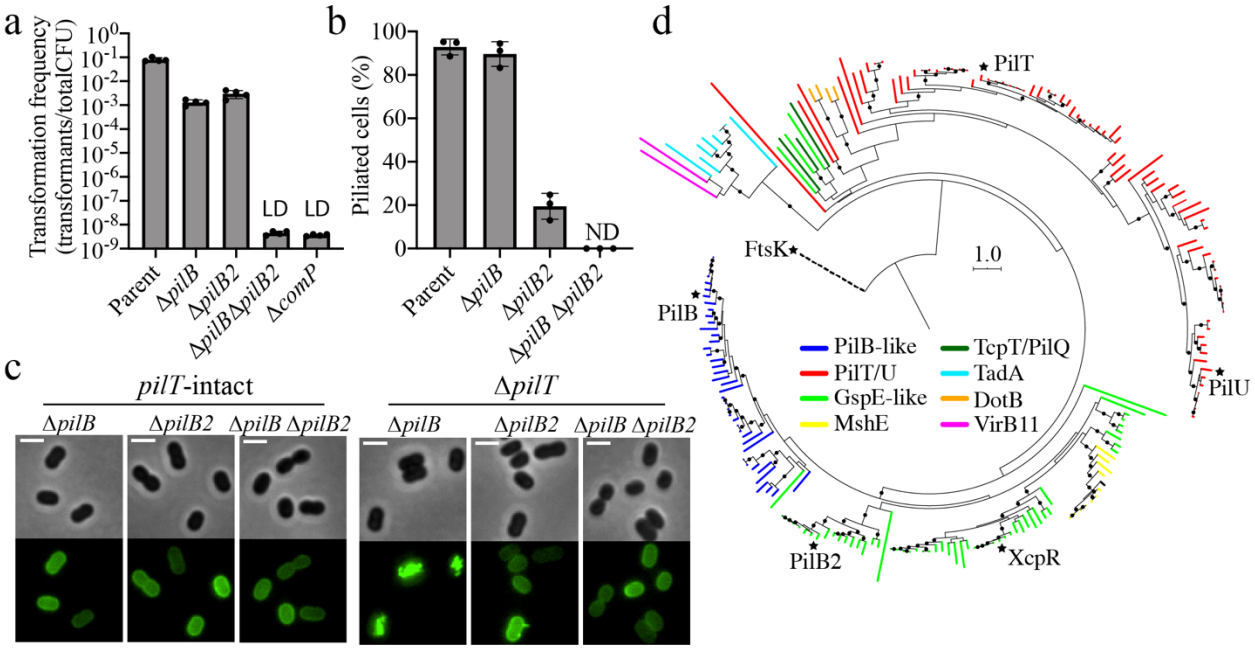

Figure 3. PilB2 is a phylogenetically distinct PilB homologue that is required for efficient T4P extension in *A. baylyi*. (**a**) Natural transformation assays of indicated strains. Each data point represents a biological replicate and bar graphs indicate the mean ± SD. LD, limit of detection. (**b**) Percent of piliated cells in *pilT* mutant populations of indicated strains. Each data point represents an independent, biological replicate and bar graphs indicate the mean ± SD. For each biological replicate, a minimum of 70 total cells were assessed. ND, no pili detected. (**c**) Representative images of indicated strains labeled with AF488-mal with background fluorescence subtracted. Scale bars, 2 μm. (**d**) A rooted phylogeny of PilB2 homologues found among Gammaproteobacteria. Branches are colored according to protein annotations in IMG, and nodes with boostrap values greater than or equal to 70% are indicated by black circles. Black stars are at the tips of branches representing *A. baylyi* proteins with indicated protein names.

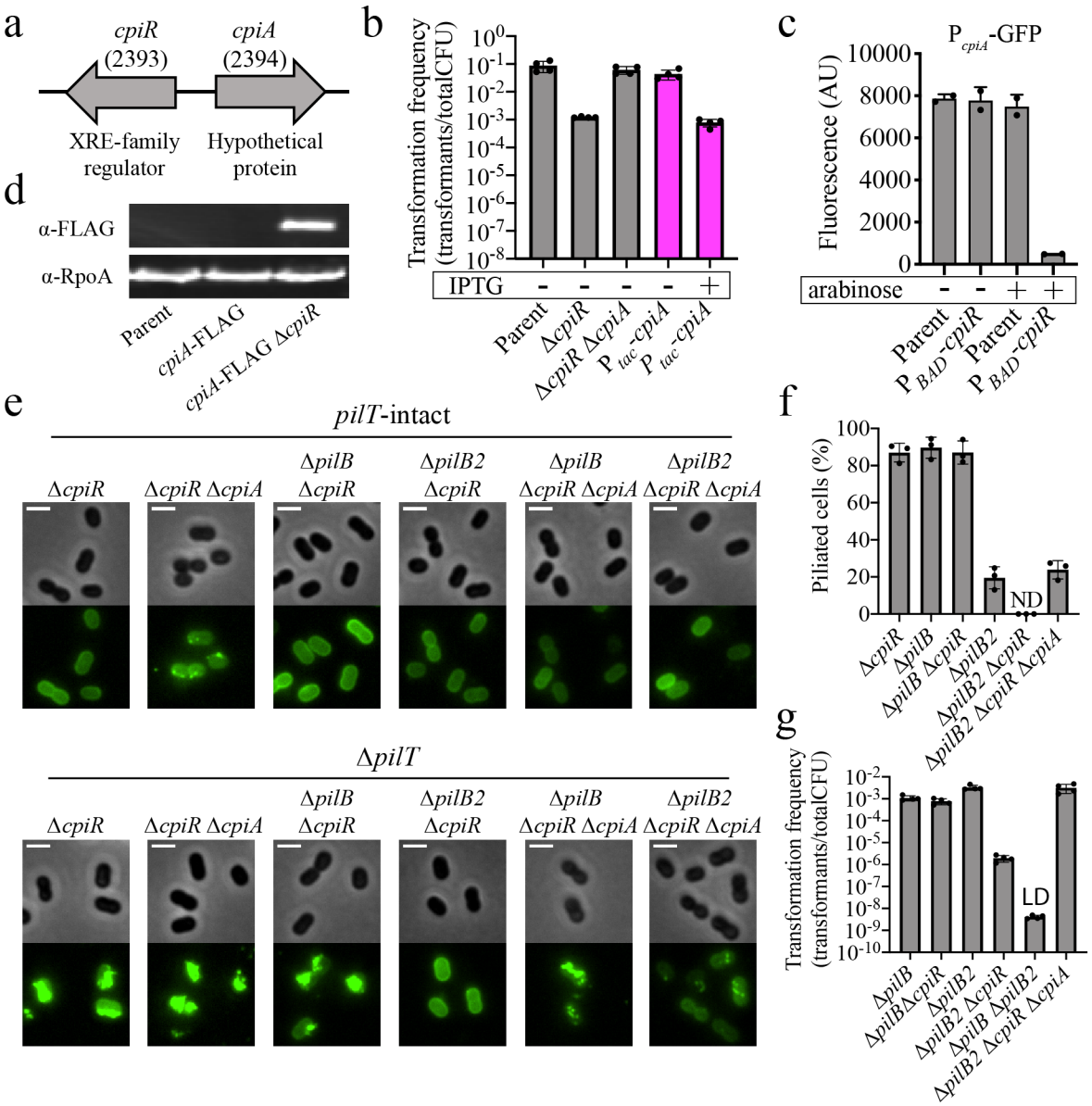

Figure 4. *A. baylyi* T4P extension is regulated by the PilB-inhibitor protein, CpiA, whose expression is controlled by the transcriptional repressor, CpiR. (**a**) Schematic *cpiRA* locus organization. (**b**) Natural transformation assays of the indicated strains performed with or without 100 μM IPTG added as indicated. Each data point represents a biological replicate and bar graphs indicate the mean ± SD. (**c**) Fluorescence intensity of *V. cholerae* strains harboring a P_{cpiA}-GFP reporter and a P_{BAD}-*cpiR* ectopic expression construct as indicated when grown with or without 0.2% arabinose as indicated. Each data point represents a biological replicate and bar graphs indicate the mean ± SD. (**d**) Western blot showing CpiA-FLAG production in the indicated strains. RpoA was detected as a loading control. (**e**) Representative images of indicated strains labeled with AF488-mal with background fluorescence subtracted. Scale bars,

524 2 μm. (**f**) Percent of piliated cells in *pilT* mutant populations of indicated strains. Each data point
525 represents an independent, biological replicate and bar graphs indicate the mean ± SD. For
526 each biological replicate, a minimum of 70 total cells were assessed. ND, no pili detected. (**g**)
527 Natural transformation assays of indicated strains. Each data point represents a biological
528 replicate and bar graphs indicate the mean ± SD. LD, limit of detection.

Supplementary Materials for

Novel mechanisms of type IV pilus regulation in *Acinetobacter baylyi*

Courtney K. Ellison[1,2*], Triana N. Dalia[3], Joshua W. Shaevitz[1*], Zemer Gitai[2*], and Ankur B. Dalia[3*]

1. Lewis-Sigler Institute for Integrative Genomics, Princeton University, Princeton, NJ
2. Department of Molecular Biology, Princeton University, Princeton, NJ
3. Department of Biology, Indiana University, Bloomington, IN

*Correspondence to: c.ellison@princeton.edu, shaevitz@princeton.edu, zgitai@princeton.edu, ankdalia@indiana.edu

This file includes:

Supplementary Figures 1-6
Supplementary Tables 1-2

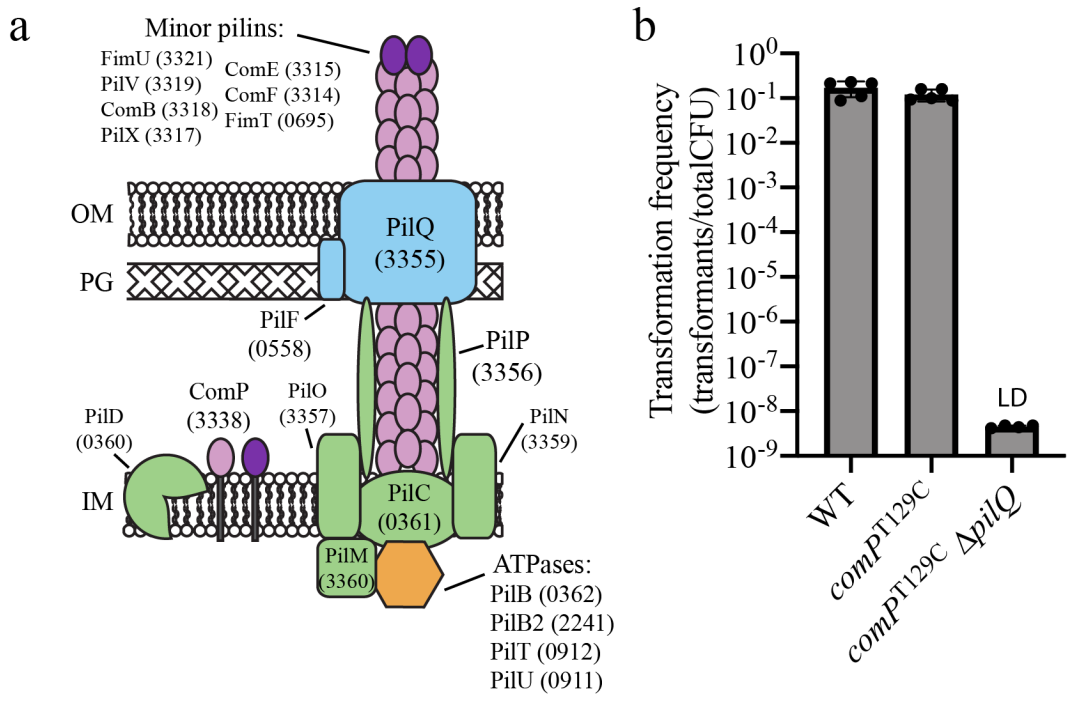

Supplemental figure 1. The strain for labeling T4P in *A. baylyi* is fully functional. (a) Schematic of assembled T4P components found in *A. baylyi*. Numbers in parentheses are ACIAD numbers associated with each component. OM, outer membrane; PG, peptidoglycan; IM, inner membrane. (b) Natural transformation assays of indicated strains. Each data point represents a biological replicate and bar graphs indicate the mean ± SD. The transformation frequency of the Δ*pilQ* strain was below the limit of detection, indicated by LD.

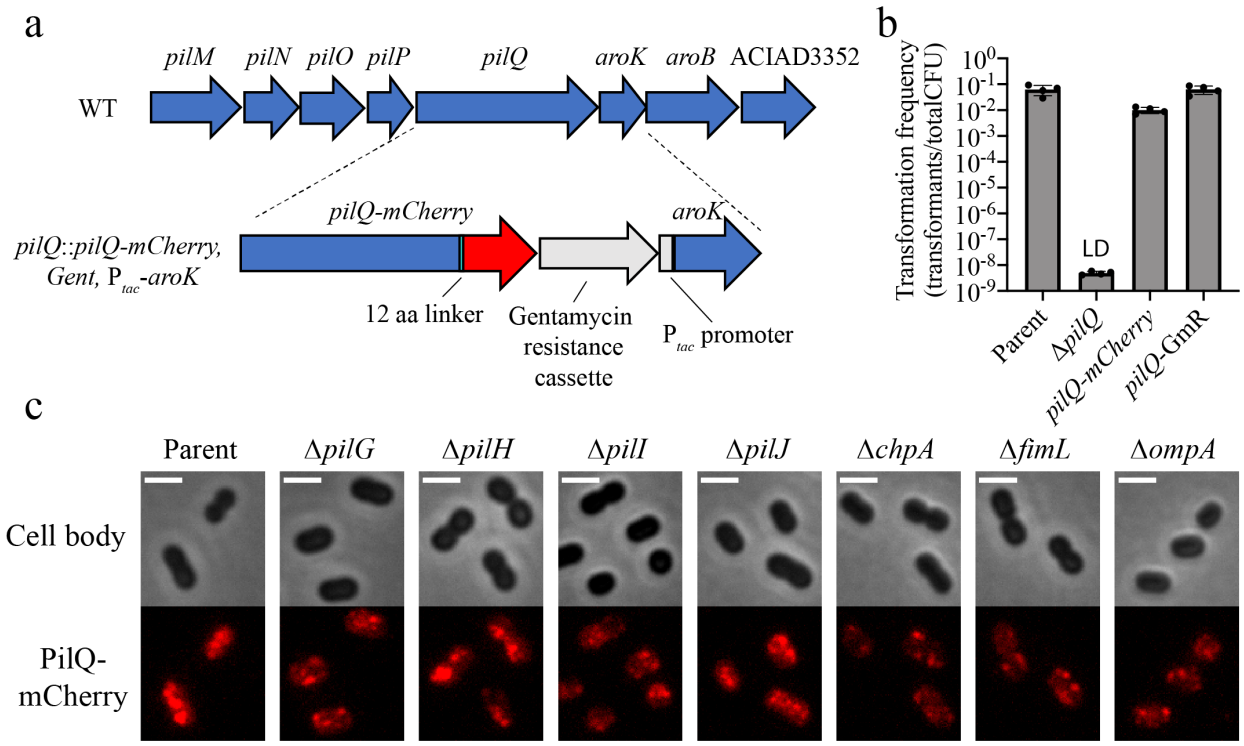

Supplemental figure 2. PilQ-mCherry localizes to the long-axis of the cell dependent on components of the Pil-Chp pathway. (a) Schematic of *pilQ-mCherry* gene locus. Attempts to make *pilQ-mCherry* by natural transformation without a selective marker were unsuccessful, and we thus added a gentamycin resistance cassette downstream of *pilQ*. Because *pilQ* is in an operon with the essential gene *aroK* immediately downstream, we added a constitutively active P_{tac} promoter to drive *aroK* expression. (b) Natural transformation assays of indicated strains. The *pilQ*-GmR control strain contains the same GmR-P_{tac} marker downstream of PilQ present in *pilQ-mCherry*, but PilQ is untagged in this background. Each data point represents a biological replicate and bar graphs indicate the mean ± SD. The transformation frequency of the Δ*pilQ* strain was below the limit of detection, indicated by LD. (c) Representative images of indicated PilQ-mCherry strains with background fluorescence subtracted. Scale bars, 2 μm.

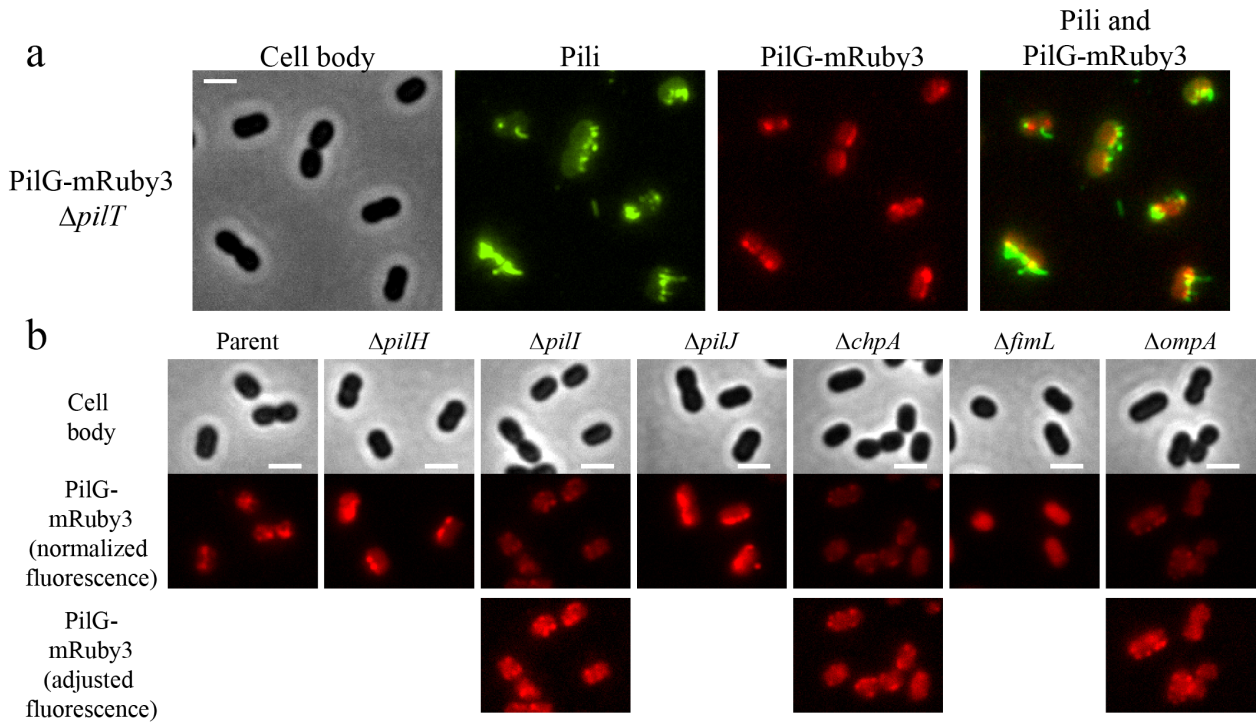

Supplemental figure 3. PilG-mRuby3 localizes at the base of T4P, and its expression is reduced in Pil-Chp mutants. (a) Representative image of PilG-mRuby3 Δ*pilT* strain labeled with AF488-mal with background fluorescence subtracted. (b) Representative images of PilG-mRuby3 localization in indicated strains with background fluorescence subtracted. Images in (b) are identical to images shown in Figure 1e, except with altered fluorescence lookup tables (LUT). Normalized fluorescence images have the same fluorescence LUT across strains, while adjusted fluorescence images have LUTs adjusted for protein visibility to show PilG-mRuby3 localization patterns. Scale bars, 2 μm.

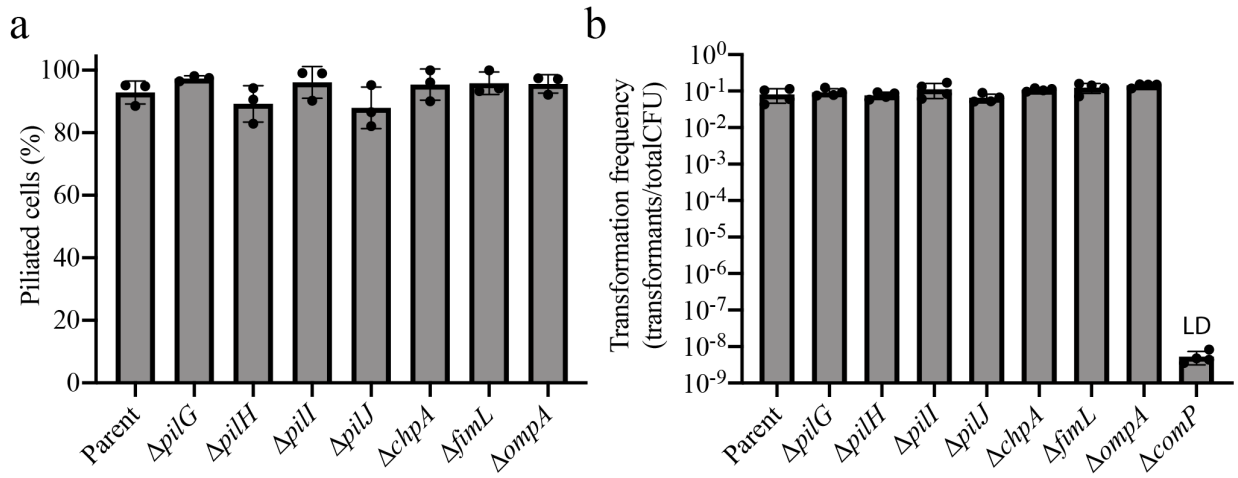

Supplemental figure 4. Pil-Chp mutants are unimpaired in T4P synthesis and are not required for natural transformation. (a) Percent of piliated cells in *pilT* mutant populations of indicated strains. Each data point represents an independent, biological replicate and bar graphs indicate the mean ± SD. For each biological replicate, a minimum of 70 total cells were assessed. (b) Natural transformation assays of indicated strains. Each data point represents a biological replicate and bar graphs indicate the mean ± SD. The transformation frequency of the Δ*comP* strain was below the limit of detection, indicated by LD.

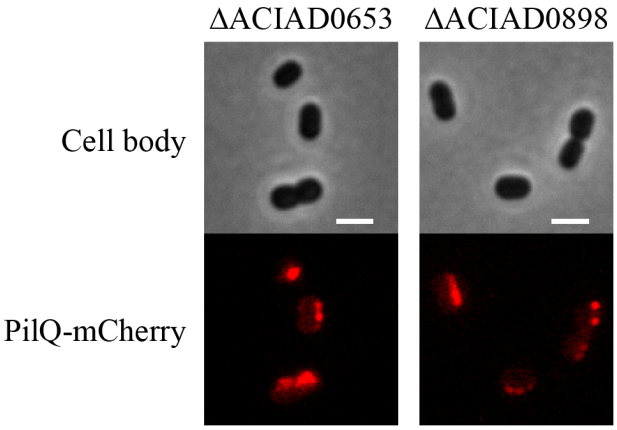

Supplemental figure 5. Other OmpA domain-containing proteins do not affect pilus machinery localization. Representative images of indicated PilQ-mCherry strains with background fluorescence subtracted. Scale bars, 2 μm.

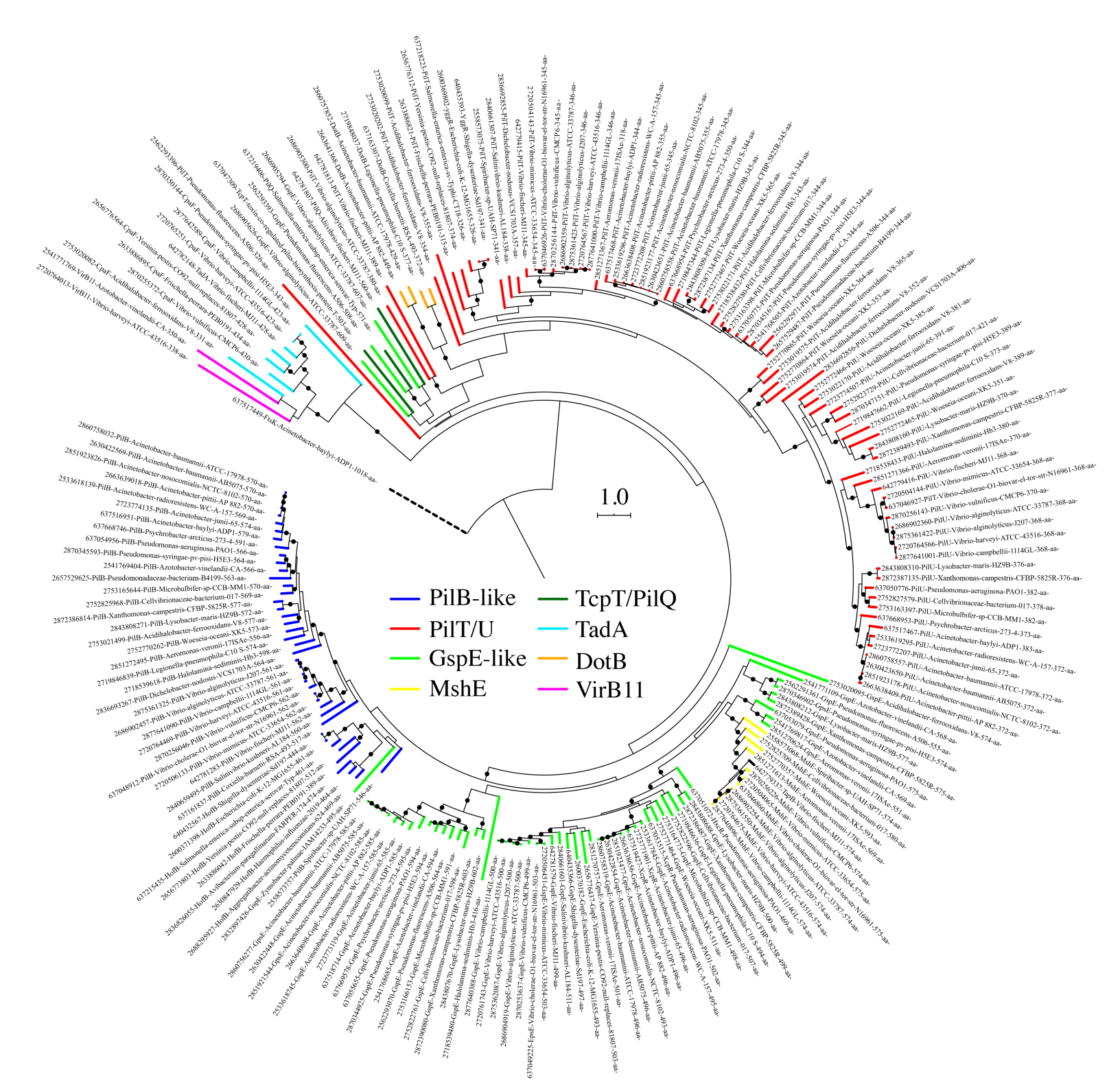

Supplemental figure 6. PilB2 clusters with a group of other GspE-like proteins that are distinct from PilB proteins. A rooted phylogeny of PilB2 homologues shown in Figure 3d with labels. Labels indicate IMG GeneID, annotated protein name, species, protein size. Nodes with boostrap values greater than or equal to 70% are indicated by black circles.

Supplementary table 1. Bacterial strains used in this study.

CE#	ZG#	TND/ SAD#	Strain name in manuscript	Genotype	Figure ('S' denotes supplemental figure)
CE1		SAD631	Wildtype (WT)	*Acinetobacter baylyi* ADP1	1A, S1B
CE100		SAD2537	Pil-cys or Parent	ADP1 *comP*^{T129C}	1A, 2A, 2C, 2D, 3A, 4B, 4D, S1B, S2B, S4B
CE329	ZG1709		Δ*pilT*	ADP1 Δ*pilT*::*spec*	1A
CE317		TND0779	Pil-cys Δ*pilT* or Parent	ADP1 *comP*^{T129C} Δ*pilT*::*spec*	1A, 1C, 2A, 2C, 3B, S4A
CE2	ZG1693		Δ*pilG*	ADP1 *comP*^{T129C} Δ*pilG*	S4B
CE3	ZG1694		Δ*pilH*	ADP1 *comP*^{T129C} Δ*pilH*	S4B
CE8	ZG1695		Δ*pilI*	ADP1 *comP*^{T129C} Δ*pilI*	S4B
CE9	ZG1696		Δ*pilJ*	ADP1 *comP*^{T129C} Δ*pilJ*	S4B
CE10	ZG1697		Δ*chpA*	ADP1 *comP*^{T129C} Δ*chpA*	S4B
CE122	ZG1698		Δ*ompA*	ADP1 *comP*^{T129C} Δ*ompA*::*kan*	S4B
CE233	ZG1699		Δ*fimL*	ADP1 *comP*^{T129C} Δ*fimL*::*kan*	S4B
		TND0114	Δ*comP*	ADP1 Δ*comP*::*kan*	3A, S4B
CE6	ZG1668		Δ*pilG* Δ*pilT*	ADP1 *comP*^{T129C} Δ*pilG* Δ*pilT*::*kan*	1C, 1D, S4A
CE7	ZG1669		Δ*pilH* Δ*pilT*	ADP1 *comP*^{T129C} Δ*pilH* Δ*pilT*::*kan*	1C, 1D, S4A
CE18	ZG1670		Δ*pilI* Δ*pilT*	ADP1 *comP*^{T129C} Δ*pilI* Δ*pilT*::*kan*	1C, 1D, S4A
CE19	ZG1671		Δ*pilJ* Δ*pilT*	ADP1 *comP*^{T129C} Δ*pilJ* Δ*pilT*::*kan*	1C, 1D, S4A
CE20	ZG1672		Δ*chpA* Δ*pilT*	ADP1 *comP*^{T129C} Δ*chpA* Δ*pilT*::*kan*	1C, 1D, S4A
CE312	ZG1675		Δ*ompA* Δ*pilT*	ADP1 *comP*^{T129C} Δ*ompA*::*kan* Δ*pilT*::*spec*	1C, 1D, S4A
CE315	ZG1676		Δ*fimL* Δ*pilT*	ADP1 *comP*^{T129C} Δ*fimL*::*kan* Δ*pilT*::*spec*	1C, 1D, S4A
CE256	ZG1681		PilQ-mCherry or Parent	ADP1 *comP*^{T129C} *pilQ*::*pilQ-mCherry, gent,* P_{tac}- *aroK*	S2B, S2C
CE331	ZG1682		PilQ-GmR	ADP1 *comP*^{T129C} *pilQ*::*pilQ, gent,* P_{tac}-*aroK*	S2B

CE320	ZG1700		Δ*pilG*	ADP1 *comP*^{T129C} *pilQ*::*pilQ-mCherry, gent,* P_{tac}- *aroK* Δ*pilG*	S2C
CE321	ZG1701		Δ*pilH*	ADP1 *comP*^{T129C} *pilQ*::*pilQ-mCherry, gent,* P_{tac}- *aroK* Δ*pilH*	S2C
CE322	ZG1702		Δ*pilI*	ADP1 *comP*^{T129C} *pilQ*::*pilQ-mCherry, gent,* P_{tac}- *aroK* Δ*pilI*	S2C
CE323	ZG1703		Δ*pilJ*	ADP1 *comP*^{T129C} *pilQ*::*pilQ-mCherry, gent,* P_{tac}- *aroK* Δ*pilJ*	S2C
CE324	ZG1704		Δ*chpA*	ADP1 *comP*^{T129C} *pilQ*::*pilQ-mCherry, gent,* P_{tac}- *aroK* Δ*chpA*	S2C
CE325	ZG1705		Δ*ompA*	ADP1 *comP*^{T129C} *pilQ*::*pilQ-mCherry, gent,* P_{tac}- *aroK* Δ*ompA*::*kan*	S2C
CE326	ZG1706		ΔACIAD0653	ADP1 *comP*^{T129C} *pilQ*::*pilQ-mCherry, gent,* P_{tac}- *aroK* Δ ACIAD0653::*kan*	S5
CE327	ZG1707		ΔACIAD0898	ADP1 *comP*^{T129C} *pilQ*::*pilQ-mCherry, gent,* P_{tac}- *aroK* Δ ACIAD0898::*kan*	S5
CE328	ZG1708		Δ*fimL*	ADP1 *comP*^{T129C} *pilQ*::*pilQ-mCherry, gent,* P_{tac}- *aroK* Δ*fimL*::*kan*	S2C
CE17	ZG1686		Parent	ADP1 *comP*^{T129C} *pilG*::*pilG-mRuby3*	1E, S3B
CE40	ZG1687		Δ*chpA*	ADP1 *comP*^{T129C} *pilG*::*pilG-mRuby3* Δ*chpA*	1E, S3B
CE127	ZG1688		Δ*ompA*	ADP1 *comP*^{T129C} *pilG*::*pilG-mRuby3* Δ*ompA*::*kan*	1E, S3B
CE257	ZG1689		Δ*fimL*	ADP1 *comP*^{T129C} *pilG*::*pilG-mRuby3* Δ*fimL*::*chlor*	1E, S3B
CE261	ZG1690		Δ*pilI*	ADP1 *comP*^{T129C} *pilG*::*pilG-mRuby3* Δ*pilI*	1E, S3B
CE341	ZG1691		Δ*pilH*	ADP1 *comP*^{T129C} *pilG*::*pilG-mRuby3* Δ*pilH*	1E, S3B

CE342	ZG1692		Δ*pilJ*	ADP1 *comP*^{T129C} *pilG*::*pilG-mRuby3* Δ*pilJ*	1E, S3B
CE25	ZG1736		PilG-mRuby3 Δ*pilT*	ADP1 *comP*^{T129C} *pilG*::*pilG-mRuby3* Δ*pilT*::*kan*	S3A
CE150	ZG1680		Δ*pilC*	ADP1 *comP*^{T129C} Δ*pilC*	2C, 2D
CE16	ZG1678		Δ*pilY1*	ADP1 *comP*^{T129C} Δ*pilY1*	2C, 2D
CE66	ZG1679		Δ*pilQ*	ADP1 *comP*^{T129C} Δ*pilQ*	2C, 2D, S1B, S2B
CE286		TND2544	Δ*comEA*	ADP1 *comP*^{T129C} Δ*comEA*::*kan*	2C, 2D
CE287		TND2546	Δ*comEC*	ADP1 *comP*^{T129C} Δ*comEC*::*kan*	2C, 2D
CE289		TND2556	Δ*comM*	ADP1 *comP*^{T129C} Δ*comM*::*kan*	2C, 2D
CE22	ZG1683		Δ*pilB*	ADP1 *comP*^{T129C} Δ*pilB*	3A, 3C, 4G
CE67	ZG1685		Δ*pilB2*	ADP1 *comP*^{T129C} Δ*pilB2*	3A, 3C, 4G
CE54	ZG1684		Δ*pilB* Δ*pilB2*	ADP1 *comP*^{T129C} Δ*pilB* Δ*pilB2*::*kan*	3A, 3C, 4G
CE310	ZG1673		Δ*pilB* Δ*pilT*	ADP1 *comP*^{T129C} Δ*pilB* Δ*pilT*::*spec*	3B, 3C, 4F
CE311	G1674		Δ*pilB2* Δ*pilT*	ADP1 *comP*^{T129C} Δ*pilB2* Δ*pilT*::*spec*	3B, 3C, 4F
CE316	ZG1677		Δ*pilB* Δ*pilB2* Δ*pilT*	ADP1 *comP*^{T129C} Δ*pilB* Δ*pilB2*::*kan* Δ*pilT*::*spec*	3B, 3C
CE263		TND1201	Δ*cpiR*	ADP1 *comP*^{T129C} Δ*cpiR*::*kan*	4B, 4E
CE264		SAD2792	Δ*cpiR* Δ*cpiA*	ADP1 *comP*^{T129C} Δ*cpiRA*::*kan*	4B, 4E
		TND2260	P_{tac}-*cpiA*	ADP1 *comP*^{T129C} igACIAD0096-ACIAD0098::*Cm*^{R}-P_{tac}-*cpiA*	4B
		TND2093	P_{cpiA}-GFP Parent	*V. cholerae* E7946 *Sm*^{R} Δ*lacZ*::*SpecR*-P_{cpiA}-*gfp*	4C
		TND2126	P_{cpiA}-GFP P_{BAD}-*cpiR*	*V. cholerae* E7946 *Sm*^{R} Δ*lacZ*::*SpecR*-P_{cpiA}-*gfp* ΔVCA0692::*Carb*^{R}-P_{BAD}-*cpiR*	4C
		TND1335	*cpiA*-FLAG	ADP1 *comP*^{T129C} *cpiA*-3X FLAG	4D

		TND1284	*cpiA*-FLAG Δ*cpiR*	ADP1 *comP*^{T129C} *cpiA*-3X FLAG Δ*cpiR*::*kan*	4D
CE282		SAD2808	Δ*pilB* Δ*cpiR*	ADP1 *comP*^{T129C} Δ*pilB* Δ*cpiR*::*kan*	4E, 4G
CE283		SAD2806	Δ*pilB2* Δ*cpiR*	ADP1 *comP*^{T129C} Δ*pilB2* Δ*cpiR*::*kan*	4E, 4G
CE284		SAD2809	Δ*pilB* Δ*cpiR* Δ*cpiA*	ADP1 *comP*^{T129C} Δ*pilB* Δ*cpiRA*::*kan*	4E
CE285		SAD2807	Δ*pilB2* Δ*cpiR* Δ*cpiA*	ADP1 *comP*^{T129C} Δ*pilB2* Δ*cpiRA*::*kan*	4E, 4G
CE265		SAD2645	Δ*cpiR* Δ*pilT*	ADP1 *comP*^{T129C} Δ*cpiR*::*kan* Δ*pilT*::*spec*	4E, 4F
CE266		SAD2810	Δ*cpiR* Δ*cpiA* Δ*pilT*	ADP1 *comP*^{T129C} Δ*cpiRA*::*kan* Δ*pilT*::*spec*	4E
CE302		SAD2822	Δ*pilB* Δ*cpiR* Δ*pilT*	ADP1 *comP*^{T129C} Δ*pilB* Δ*cpiR*::*kan* Δ*pilT*::*spec*	4E, 4F
CE303		SAD2820	Δ*pilB2* Δ*cpiR* Δ*pilT*	ADP1 *comP*^{T129C} Δ*pilB2* Δ*cpiR*::*kan* Δ*pilT*::*spec*	4E, 4F
CE304		SAD2823	Δ*pilB* Δ*cpiR* Δ*cpiA* Δ*pilT*	ADP1 *comP*^{T129C} Δ*pilB* Δ*cpiRA*::*kan* Δ*pilT*::*spec*	4E
CE305		SAD2821	Δ*pilB2* Δ*cpiR* Δ*cpiA* Δ*pilT*	ADP1 *comP*^{T129C} Δ*pilB2* Δ*cpiRA*::*kan* Δ*pilT*::*spec*	4E, 4F

CE strains available upon request from CKE, ZG strains available upon request from ZG, TND or SAD strains available upon request from ABD.

Supplementary table 2. Primers used for strain construction.

Primer name	Primer sequence 5' → 3' (overlapping regions underlined, point mutations in bold)	Description
DOG0175	AAACTATCCAGATAAGGGAAAGC	comP F1
CEdalia87	GAAGTTGTCGTACATTTCCA**ACA**TACAGCGCCACTAGCATATG	comPT129C R1
CEdalia88	CATATGCTAGTGGCGCTGTA**TGT**TGGAAATGTACGACAACTTC	comPT129C F2
DOG0178	AGGATCTGTAATGACGGGTTGAG	comP R2
DOG0176	GTCGACGGATCCCCGGAATCATAAAATTTCTCCACCAATGTTG	ΔcomP R1
DOG0177	GAAGCAGCTCCAGCCTACATGATAGTAGTACTATATGGCTTTAAAAG	ΔcomP F2
ABD123	ATTCCGGGGATCCGTCGAC	AbR cassette F
ABD124	TGTAGGCTGGAGCTGCTTC	AbR cassette R
BBC1934	GTTACAAAGTCAGGGACGTAAAG	ΔpilT F1
BBC1935	GTCGACGGATCCCCGGAATATCCATATTTTCCCCGAAGATCG	ΔpilT R1
BBC1936	GAAGCAGCTCCAGCCTACATAAGAATAACGCTACTCGATCTG	ΔpilT F2
BBC1939	GGTATTCAGATTGATCGTCAGTTAG	ΔpilT R2
CE31	GCTGTTTGATTTTATCCAGAACCTTG	ΔpilG F1
CE61	TGACGTGATTACGAATTGCGGTGATTTTGATCACTTTGGATTTGTCTTCC	ΔpilG R1
CE62	GGAAGACAAATCCAAAGTGATCAAAATCACCGCAATTCGTAATCACGTCA	ΔpilG F2
CE34	GCGCTGTAATTACAATAGTGTTCGGA	ΔpilG R2 and pilG-mRuby3 R2
CE37	GGTGGTACGCAGTTGTGGTAAAAT	ΔpilH F1 and pilG-mRuby3 F1
CE63	ATCATCCGTATGAATATATTGCTGGATTGAATCATCAACAATCAAAATACGTGCCA	ΔpilH R1
CE64	TGGCACGTATTTTGATTGTTGATGATTCAATCCAGCAATATATTCATACGGATGAT	ΔpilH F2
CE40	GGCAACTCAATTCAAACTGATGTACTT	ΔpilH R2
CE101	TTCAACGCTCATTCGTTGCCAT	ΔpilI F1
CE102	ATCAATATTGTGAAGCATTCATAAAATCTGTCAAACCAGCAGATGTGGTTGC	ΔpilI R1
CE103	GCAACCACATCTGCTGGTTTGACAGATTTTATGAATGCTTCACAATATTGAT	ΔpilI F2
CE104	CAGTTGACTGGTTACTGGTTCTGC	ΔpilI R2
CE107	GGTTTTTCCAGTTTTTAATGCTGCC	ΔpilJ F1

CE108	TCAGATGCAAAATCAAGCTTATACGTCGCTTTATTTTTTTTCCGATTGATTGA	ΔpilJ R1
CE109	TCAATCAATCGGAAAAAAAATAAAGCGACGTATAAGCTTGATTTTGCATCTGA	ΔpilJ F2
CE110	CCGAACAGTACGCTGCAATC	ΔpilJ R2
CE29	AATATCTTGTCGCCGATTCATTGAAA	ΔchpA F1
CE113	GGTTTTGGCTATGTTTAATCGCTTTCGTCTCTATAAGATGATTTACTTGTGCA	ΔchpA R1
CE114	TGCACAAGTAAATCATCTTATAGAGACGAAAGCGATTAAACATAGCCAAAACC	ΔchpA F2
CE115	CTGTATTTTGATGCAATGTTGGAGATT	ΔchpA R2
CE502	AATGGTGGGCCGTGAAAAAGC	ΔompA F1
CE503	GTCGACGGATCCCCGGAATAGTAGCAAGTGCAATACGACTCAATTTc	ΔompA R1
CE504	GAAGCAGCTCCAGCCTACAGTTCAACCTGGTCAACAAGCTCC	ΔompA F2
CE505	CCAGATCAGATACCAGATCAGGTGATTAT	ΔompA R2
CE735	GTGCACTGGGGATATCTGCACT	ΔfimL F1
CE736	GTCGACGGATCCCCGGAATATCGAAGCGAATAGAAACTTGTGAAGAC	ΔfimL R1
CE737	GAAGCAGCTCCAGCCTACAAACGCCTCCCAATTTCAATCAACG	ΔfimL F2
CE738	TGCTAACAGAATTGTATGTGTCTACGCC	ΔfimL R2
CE590	ATGAGAACAGATTTTAACGTTTTTACGACTGG	PilQ-mCherry up F
CE196	GAACCAGCAGCTGAACCAGCTGAACCATGATTTCCAACAATAGTGTCATTAACTATTCG	PilQ-mCherry up R
CE197	TTCAGCTGCTGGTTCAGGTGAATTTATGGTTTCCAAGGGCGAGGA	PilQ-mCherry mCherry region F
CE198	TTACTTGAATTAAAACTATATTATTTGTACAGCTCATCCATGCCA	PilQ-mCherry mCherry region R
CE637	TATAGTTTTAATTCAAGTAATTCAATAGGTGACTCCATTCCGGGGATCCGTCGAC	PilQ-mCherry AbR region F1
CE593	TCGTTGCTGCTGCGTAACATGCGAAACTATCCTCATCCTGTCTCTTG	PilQ-mCherry AbR region R1
CE594	CAGGATGAGGATAGTTTCGCATGTTACGCAGCAGCAACGATG	PilQ-mCherry AbR region F2
CE595	GGAACTTCAAGATCCCCTTATTAGGTGGCGGTACTTGGGTC	PilQ-mCherry GmR region R2

CE596	GACCCAAGTACCGCCACCTAATAAGGGGATCTTGAAGTTCCTATTCCG	PilQ-mCherry Ptac region F
CE336	GCTTAATTACCTCCTAATTGAATTCCTAGGC	PilQ-mCherry Ptac region R
CE638	GGAATTCAATTAGGAGGTAATTAAGCTTGCCAAGCAAAGAGTTTGACACC	PilQ-mCherry down F
CE592	TCTAATGCCGCTGCACTGTCAC	PilQ-mCherry down R
CE546	CCAGATCTCTACGCATTTCACCG	ΔACIAD0653 F1
CE547	GTCGACGGATCCCCGGAATGACCCCAAGAATAGATATTTTGATTGAGTTGT	ΔACIAD0653 R1
CE548	GAAGCAGCTCCAGCCTACACGCGTTGCAATTGTAATCGTTCC	ΔACIAD0653 F2
CE549	GTAGAAGGGTCTCATGTTGCGGG	ΔACIAD0653 R2
CE552	CACAATACGTCCCAGCAATTGAAAC	ΔACIAD0898 F1
CE553	GTCGACGGATCCCCGGAATGACTAGTGCACGCATTGCATGC	ΔACIAD0898 R1
CE554	GAAGCAGCTCCAGCCTACAGAGATTAGCATTTACGAACGTCAATAAGCG	ΔACIAD0898 F2
CE555	CGACACATGTTTGCTCTGCATCC	ΔACIAD0898 R2
CE146	TTCACCTGAACCAGCAGCTGAACCAGCTGAACCTACACTGACGTGATTACGAATTGCG	pilG-mRuby3 R1
CE147	TGGTTCAGCTGCTGGTTCAGGTGAATTTATGGTATCTAAGGGTGAAGAATTGATTAAGG	mRuby3 F
CE148	TTACTTATATAATTCATCCATTCCACCCCCAAG	mRuby3 R
CE149	GGGTGGAATGGATGAATTATATAAGTAACACGATATTGTTTTGAGGTCTTTATGGCAC	pilG-mRuby3 F2
CE389	TCAGGAAGTTGCCTGAACCTGA	ΔpilC F1
CE390	ACAGAGCCCATTTGGAAAATTGGTGGCATTACTTGCGTTTTTTTTGCT	ΔpilC R1
CE391	AGCAAAAAAAACGCAAGTAATGCCACCAATTTTCCAAATGGGCTCTGT	ΔpilC F2
CE392	TTGAAAAGCTGGCTGGCCTTC	ΔpilC R2
CE136	TTGGTCGATAATGCAGATCAGCT	ΔpilY1 F1
CE137	GGGGTGCTTTGCTCATACCATTTTAAGAGATACTGAGTGTATATCGATTTTTTCAT	ΔpilY1 R1
CE138	ATGAAAAAATCGATATACACTCAGTATCTCTTAAAATGGTATGAGCAAAGCACCCC	ΔpilY1 F2

CE139	GCAGGGATATCAGATTTTAACTGTGC	ΔpilY1 R2
CE85	AATAAGAGCGAATAGCAAACTAATTGTCG	ΔpilQ F1
CE340	TTTCCAACAATAGTGTCATTAACTATTCGAGTCGTAAAAACGTTAAAATCTGTTCTCAT	ΔpilQ R1
CE341	ATGAGAACAGATTTTAACGTTTTTACGACTCGAATAGTTAATGACACTATTGTTGGAAA	ΔpilQ F2
CE88	AGCGTATAACGATCAATTACTTCGC	ΔpilQ R2
BBC1891	AATCACTTGAAGTGCAGATTCG	ΔcomEA F1
BBC3451	GTCGACGGATCCCCGGAATATGACGTATTGACATGAATTAACC	ΔcomEA R1
BBC3452	GAAGCAGCTCCAGCCTACATAAGAGGCTGAGTCATGCTCAAAATAC	ΔcomEA F2
BBC1894	ATCTTCACCTTCTCCAAACTGG	ΔcomEA R2
DOG0180	AGTATTTGAGTTCGGGTATTATTGC	ΔcomEC F1
DOG0181	GTCGACGGATCCCCGGAATCATGGCAATGCCAGCAATC	ΔcomEC R1
DOG0182	GAAGCAGCTCCAGCCTACAAAGGGAGCGATTCATTTTAAGTTTG	ΔcomEC F2
DOG0183	TTACTCAAGCCGTTACAGTTCTG	ΔcomEC R2
DOG0140	GTTGCTGCATTTGTTCGATCTG	ΔcomM F1
DOG0141	GTCGACGGATCCCCGGAATCATACTATTATTGTTCCATTATGGTGC	ΔcomM R1
DOG0142	GAAGCAGCTCCAGCCTACATATCGCAGTGAACATAGCTAAAA	ΔcomM F2
DOG0143	ATCAGTGGTTGGGAAGGTG	ΔcomM R2
CE23	TTATGACTATCAATCTCAAGCACATGCT	ΔpilB F1
CE93	ATTCACTGGTTACACGATTAATTTCCTGAAACTTAGGTGGTGTTGTAAATGCTG	ΔpilB R1
CE94	CAGCATTTACAACACCACCTAAGTTTCAGGAAATTAATCGTGTAACCAGTGAAT	ΔpilB F2
CE26	CTTTCATGGCGTGTTTGTCGTG	ΔpilB R2
CE210	AAGCCAACCATAATCCGATTGTGAC	ΔpilB2 F1
CE328	TGGGACCACCCTTAAGACTTCTTCCCATTGTGTATCTATTTCAAAATGATATGTCAT	ΔpilB2 R1 (in frame)
CE329	ATGACATATCATTTTGAAATAGATACACAATGGGAAGAAGTCTTAAGGGTGGTCCCA	ΔpilB2 F2 (in frame)
CE213	CTCACGCCACCCAATCAAGAC	ΔpilB2 R2
CE240	GTCGACGGATCCCCGGAATTTATTTCTCCCCCACACCATTCAC	ΔpilB2 R1 (AbR disruption)

CE241	GAAGCAGCTCCAGCCTACATAAAAGGTTAGTTTAGATCTTAAGATTCACCTCAT	ΔpilB2 F2 (AbR disruption)
DOG0130	CCTCTCCACTCGTTTCTAAAGAAC	ΔcpiR or ΔcpiA or cpiA-3X FLAG F1
DOG0131	GTCGACGGATCCCCGGAATCATAAGCCGATACTATCTGGATGG	ΔcpiR R1
DOG0132	GAAGCAGCTCCAGCCTACAGAAGTTCAATGTCAGTTAAAACATC	ΔcpiR F2
DOG0133	GACGTTGATTACGTAAATTTAATTCG	ΔcpiR or ΔcpiA or cpiA-3X FLAG R2
BBC921	GTCGACGGATCCCCGGAATTTGATCACTTACTAATTTCATTATCATTTAAATG	ΔcpiA R1
BBC922	GAAGCAGCTCCAGCCTACATAAAAAAGGACTGATTTCTCAGCCC	ΔcpiA F2
BBC2565	TCCACCACTTCCACCTGCATTTTCATGAAACACTTGCTGC	cpiA-3X FLAG R1
BBC2570	GCAGGTGGAGCAGGTGGATAAAAAAGGACTGATTTCTCAGCCC	cpiA-3X FLAG F2
BBC2272	GCAGGTGGAAGTGGTGGAGATTATAAAGACCATGATGGTGACTACAAGGATCACGACATTGATTATAAGGATGACGATGACAAAGCAGGTGGAGCAGGTGGA	3X FLAG MIDDLE F
BBC2273	TCCACCTGCTCCACCTGCTTTGTCATCGTCATCCTTATAATCAATGTCGTGATCCTTGTAGTCACCATCATGGTCTTTATAATCTCCACCACTTCCACCTGC	3X FLAG MIDDLE R
DOG0229	CAATTTCACACAGGATCCCGGGAGGAGGTAACGTAATGATAATGAAATTAGTAAGTGATCAAATTC	Amplify *cpiA* for P_{tac}-*cpiA* construct F
DOG0230	TGTAGGCTGGAGCTGCTTCTTAATTTTCATGAAACACTTGCTGC	Amplify *cpiA* for P_{tac}-*cpiA* construct R
BBC3072	CACCATTATGATGGCAATCGTATGATTCGAAGTATGTGAAAAATCTGC	Amplify P_{cpiA} for P_{cpiA}-GFP F
BBC3074	CCCGGGATCCTGTGTGAAATTGACTAGCAGTATTGTATTACAAAACTTTTG	Amplify P_{cpiA} for P_{cpiA}-GFP R
BBC3075	CAATTTCACACAGGATCCCGGGAGGAGGTCGGCTTATGGATATAGGTCGC	Amplify *cpiR* for P_{BAD}-*cpiR* construct F
BBC2560	TGTAGGCTGGAGCTGCTTCTTACTTTTTAGTGTCTATCAAAGTAAAAATGAGATG	Amplify *cpiR* for P_{BAD}-*cpiR* construct R